Analytical Biochemistry 629 (2021) 114269

Contents lists available at ScienceDirect

Analytical Biochemistry

journal homepage: www.elsevier.com/locate/yabio

Spectral decomposition of iron-sulfur clusters

Isaiah O. Betinol [1], Serge Nader [1], Sheref S. Mansy [*]

Department of Chemistry, University of Alberta, 11227 Saskatchewan Drive, Edmonton, AB, T6G 2G2, Canada

ARTICLE INFO

Keywords:
Iron-sulfur cluster
Prebiotic chemistry
Spectral decomposition
Microsoft excel

ABSTRACT

The near universal availability of UV–Visible spectrophotometers makes this instrument a highly exploited tool for the inexpensive, rapid examination of iron-sulfur clusters. Yet, the analysis of iron-sulfur cluster reconstitution experiments by UV–Vis spectroscopy is notoriously difficult due to the presence of broad, ill-defined peaks. Other types of spectroscopies, such as electron paramagnetic resonance spectroscopy and Mössbauer spectroscopy, are superior in characterizing the type of cluster present and their associated electronic transitions but require expensive, less readily available equipment. Here, we describe a tool that utilizes the accessible and convenient platform of Microsoft Excel to allow for the semi-quantitative analysis of iron-sulfur clusters by UV–Vis spectroscopy. This tool, which we call Fit-FeS, could potentially be used to additionally decompose spectra of solutions containing chromophores other than iron-sulfur clusters.

1. Introduction

Iron-sulfur clusters are ancient cofactors that mediate chemistry within central metabolism [1]. Iron-sulfur clusters most commonly exist in three primarily cysteine ligated states, including mononuclear (i.e. [1Fe–0S]), [2Fe–2S], and [4Fe–4S] clusters. However, distinguishing between the different types of clusters by inexpensive methods, such as UV–Visible spectroscopy, can be difficult due to their notoriously broad absorption peaks. These broad bands arise from the large number of electronic transitions, which increase with increasing nuclearity of the cluster, culminating with the relatively featureless spectrum of [4Fe–4S] clusters [2]. Therefore, initial analyses of iron-sulfur clusters typically rely on qualitative comparisons of UV–vis spectra with previously published reports. While such an approach often gives satisfactory results for iron-sulfur proteins, the situation can be more complex for iron-sulfur peptides, because the same iron-sulfur peptide can frequently coordinate different types of clusters [3]. The ability to quickly characterize a peptide-bound cluster would be invaluable in monitoring reaction processes when forming clusters in situ [4]. Though rarer, some proteins exhibit similar characteristics of interconversion [5].

To better asses the types of clusters present in a heterogenous mixture, a spectral decomposition program is desirable. The use of spectral decomposition avoids the assumption that only one type of cluster is present in solution. Alternative methods do exist [2], and commercial software (e.g. PeakFit, a|e 1.2, and MatLab) [6–8] that can handle well the needed spectral decomposition are available; however, many laboratories do not typically use or do not have access to these options. A good solution for some would be to use free statistical software, such as R [9], but many are not familiar with the programming language. Here we provide an easy-to-use automated spreadsheet that utilizes the Microsoft Excel macro function and the Solver add-in [10] to analyze solutions of iron-sulfur clusters. These tools are free and included with the standard Microsoft Office package. Although Microsoft Excel is a commercial software, the availability of the Microsoft Office suite is widespread across academia and industry, and most researchers are accustomed to using these programs. The Microsoft Excel Solver add-in is capable of fitting curves and spectra [11–13] and Microsoft Excel macros are a well-established tool for scientific data analysis [14–16]. Our spreadsheet, called Fit-FeS, allows users to statistically analyze a series of iron-sulfur cluster spectra with the click of a button. Analysis of spectra collected over time shows the formation and degradation of different iron-sulfur species throughout the course of a reaction.

This tool is not meant, nor can it, substitute for analyses with more advanced spectroscopies, such as EPR and Mössbauer spectroscopies. However, more can be learned quickly and cheaply from the ubiquitous UV–Vis spectrophotometer than is typically gained, if simple fitting tools, as we provide here, are available. Also, the speed of spectral acquisition with UV–Vis spectrophotometers opens up possibilities in monitoring reactions over time that would either not be possible or

* Corresponding author.
E-mail addresses: ibetinol@ualberta.ca (I.O. Betinol), serge.nader@ualberta.ca (S. Nader), sheref.mansy@ualberta.ca (S.S. Mansy).
[1] These authors contributed equally.

https://doi.org/10.1016/j.ab.2021.114269
Received 16 April 2021; Received in revised form 28 May 2021; Accepted 31 May 2021
Available online 3 June 2021

would be cumbersome and costly by other techniques. Further, Fit-FeS will likely facilitate the analysis of chromophores other than iron-sulfur clusters.

2. Materials and methods

All reagents were from Sigma-Aldrich or Aapptec and used without further purification, unless otherwise noted. All peptides were synthesized according to standard solid-phase peptide synthesis procedures [4] or purchased from LifeTein LLC. Synthesis was performed under a N_2 atmosphere using Schlenk lines and Schlenk glassware. Stock solutions were prepared with deoxygenated water that was made by distilling deionized ultrapure water (Synergy UV Water Purification System) under a N_2 atmosphere. Stock solutions were stored in anaerobically sealed glass vials until further use. UV–vis absorption spectra were collected with an Agilent Cary 3500 UV–Vis spectrophotometer (Integration = 0.02 s, interval = 1 nm) with sealed anaerobic quartz cuvettes (path length = 0.5 cm). Parafilm was wrapped around the caps of the cuvettes. pH measurements were made with an Orion Star A211 pH meter with pH and ATC Probes from Thermo Scientific.

2.1. Iron-sulfur cluster reconstitution

Reconstitution procedures were adapted from previous reports [3,17]. In short, stock solutions of peptide, glycylglycine, $FeCl_3{\cdot}6H_2O$, and $Na_2S{\cdot}9H_2O$ were prepared under anaerobic conditions and stored at −20 °C when not in use. For the synthesis of [4Fe–4S] clusters, peptide (5 mM concentration of cysteine) was added to a solution of 50 mM glycylglycine, and 5 M NaOH was added until the pH was 8.7. This solution was then transferred to a N_2-conditioned FireflySci quartz cuvette to which solutions of $FeCl_3$ and Na_2S were added using gas tight Hamilton syringes. Final concentrations in the cuvette were 0.4 mM $Fe^{3+}{}_{(aq)}$, and 0.8 mM hydrosulfide (HS^-). For the synthesis of the [4Fe–4S] cluster coordinated to KLCEGGCIACGACGGW, 2% (v/v) β-mercaptoethanol and 50 mM HEPES, pH 8.7 were used, as per previous reports [17], in place of glycylglycine. [2Fe–2S] and [1Fe–0S] clusters were synthesized by the same procedure as [4Fe–4S] clusters but in the absence of buffer and with different concentrations of $Fe^{3+}{}_{(aq)}$ and hydrosulfide. For the synthesis of [2Fe–2S] clusters, the final concentrations were 0.4 mM $Fe^{3+}{}_{(aq)}$ and 0.19 mM HS^-. For reconstitution of mononuclear clusters, the final concentration was 0.4 mM $Fe^{3+}{}_{(aq)}$ with no addition of Na_2S. The assembly of non-peptidyl iron sulfide followed the same procedure as for the synthesis of $[4Fe–4S]^{2+}$ peptide but without peptide added. Cluster reconstitution was monitored by UV–vis spectroscopy over time at 25 °C for up to 24 h or by a thermal assay from 25 °C to 80 °C with intervals of 5 min/5 °C.

2.2. Spectral fitting

The automated spreadsheet utilized previously published methods of spectral fitting [10–12]. Models were generated as a linear combination of reference spectra. The method of least squares was then employed to match the model to a sample spectrum, utilizing the Microsoft Excel add-in Solver (Microsoft Excel, 2016) to minimize error. The proportion of each reference was equal to the individual coefficient divided by the sum of all reference coefficients. The uncertainty calculated for each data point was the root-mean-square error of the spectral fit. The error shown in the graphs was the root-mean-square error, which was more valid, in this case, than mean-average-error. More weight was given to errors in models that fit data poorly, as such models likely indicated the presence of a species not accounted for by the reference matrix [18]. To estimate the concentrations of each species after spectral fitting, the proportional spectral contribution was multiplied by the absorbance at wavelengths where extinction coefficients were reported. The Beer-Lambert law was then employed to obtain the concentration after user input of path length and extinction coefficient. The default extinction coefficients were 7400 $M^{-1}cm^{-1}$ at 310 nm for $[1Fe–0S]^{2+}$ clusters [19], 6600 $M^{-1}cm^{-1}$ at 420 nm for $[2Fe–2S]^{2+}$ clusters [20], and 16100 $M^{-1}cm^{-1}$ at 385 nm for $[4Fe–4S]^{2+}$ clusters [21]. Excel macros were coded in Visual Basic for Applications. Detailed instructions on how to use the spreadsheet can be found in the Supporting Information. Fit-FeS and reference spectra can be found in the supplementary information and Zenodo (https://doi.org/10.5281/zenodo.4765989).

3. Results and discussion

3.1. Development of a library with peptidyl and non-peptidyl spectra

The reference library for spectral fitting contained UV–vis spectra of iron-sulfur peptides of 20 amino acids or less. UV–Vis spectra are remarkably similar between iron-sulfur proteins, peptides, and purely inorganic iron-sulfur clusters [17,22]; however, analysis of protein-based systems may be better served by reference spectra of iron-sulfur proteins. The reference $[4Fe–4S]^{2+}$ peptide (KLCEGGCIACGACGGW) was developed by the Dutton group and is often referred to as a ferredoxin maquette [17]. The previously characterized PESCKAGACSTCAGPDLTCT [20] and GCPLC [19] peptides were used to produce reference spectra for $[2Fe–2S]^{2+}$ and $[1Fe–0S]^{2+}$ clusters, respectively. After the synthesis of each cluster type coordinated to their respective peptides, each gave spectra consistent with previous reports (Figs. S1–S3).

In the absence of a chelating agent, such as a peptide or protein, iron ions and hydrosulfide readily combine to form multitudinous amounts and stoichiometries of iron sulfide species [23]. These complexes can also form from a subset of the iron and hydrosulfide ions in solution prior to coordination to peptides, or the complexes can form after the degradation of peptide coordinated cluster, as has been observed during the unfolding of proteins [24]. Therefore, we included reference spectra for the non-peptidyl complexes that form by following the same protocol for the synthesis of the $[4Fe–4S]^{2+}$ cluster coordinated to peptide but in the absence of peptide. These non-peptidyl complexes absorbed broadly across the entire spectra with sharper peaks at 450 nm and 620 nm (Fig. S4). The library of reference spectra also contained peptides in the absence of iron and hydrosulfide ions.

3.2. Fitting of iron-sulfur peptide spectra

To determine if the Solver macro could accurately determine the cluster type of an iron-sulfur peptide through spectral fitting, the previously investigated [4Fe–4S] GCIACGAC peptide was tested. This peptide was identical to the FdM-7 peptide reported by Mulholland et al. but contained an additional amino-terminal glycine. FdM-7 was shown to coordinate a $[4Fe–4S]^{2+/+}$ cluster by Mössbauer and EPR spectroscopies [25]. Spectral fitting over time following the addition of ferric chloride and sodium sulfide to a solution containing the GCIACGAC peptide showed the progressive formation of the $[4Fe–4S]^{2+}$ cluster until the reaction was complete after 6 h (Fig. 1a, Fig. S5). Early time points indicated the presence of $[1Fe–0S]^{2+}$and $[2Fe–2S]^{2+}$ clusters that then decreased as the concentration of $[4Fe–4S]^{2+}$ cluster increased. The data were consistent with the types of cluster synthesis pathways reported by Holm and colleagues [26] and peptide dynamics calculated by Szilagyi and colleagues [27], although alternative mechanisms were possible [28]. Conversely, if the reactions were monitored by the diagnostic absorption peaks of each cluster type (Fig. 1b), the data would erroneously suggest that all three types of iron-sulfur clusters increased over time. Spectral fitting with our tool Fit-FeS, which relied on algorithms available within Microsoft Excel, gave a much more accurate picture of the types of iron-sulfur clusters in solution.

To monitor the consecutive assembly of iron-sulfur clusters with a system that has been more thoroughly investigated kinetically, we next turned to iron-sulfur clusters coordinated to glutathione. The irradiation

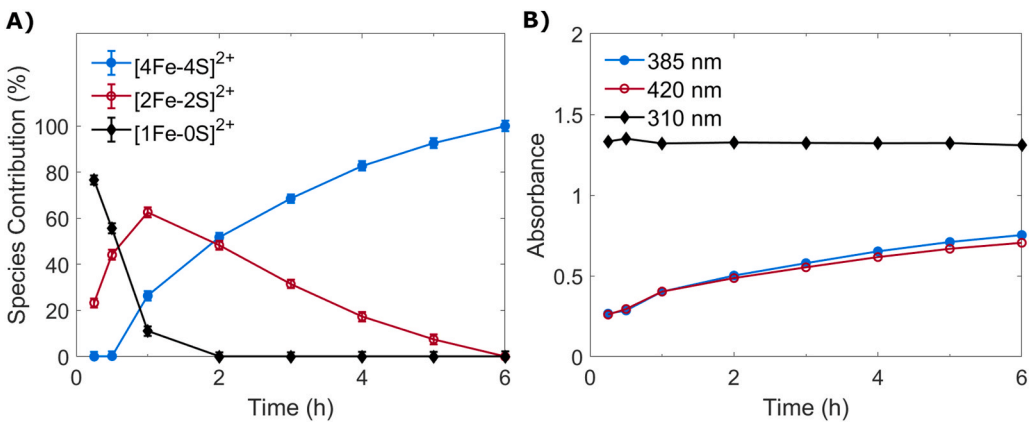

Fig. 1. Formation of a $[4Fe–4S]^{2+}$ cluster coordinated to GCIACGACG. A) Monitoring cluster formation with Fit-FeS. The reaction was initiated by the anaerobic addition of 0.8 mM Na_2S and 0.4 mM $FeCl_3$ to 1.67 mM GCIACGACG, 50 mM glycylglycine, pH 8.7. Absorption spectra were fit to a spectral library of $[1Fe–0S]^{2+}$, $[2Fe–2S]^{2+}$, and $[4Fe–4S]^{2+}$ peptides. B) Monitoring cluster formation by measuring absorbance at single wavelengths indicative of cluster type, including $[4Fe–4S]^{2+}$ (385 nm), $[2Fe–2S]^{2+}$ (420 nm), and $[1Fe–0S]^{2+}$ (310 nm) clusters. The same raw spectral data were used to generate the plots in panels a and b.

of $[1Fe–0S]^{2+}$ glutathione results in the progressive formation of $[2Fe–2S]^{2+}$ and then $[4Fe–4S]^{2+}$ cluster due to the production of hydrosulfide from the photolysis of a fraction of the glutathione tripeptides (γECG) [4]. As expected, irradiation of $[1Fe–0S]^{2+}$ glutathione with UV (254 nm) light resulted in a rapid decrease of the mononuclear species followed by a solution dominated by the presence of $[2Fe–2S]^{2+}$ cluster succeeded by absorption predominantly reflective of $[4Fe–4S]^{2+}$ cluster (Fig. 2, Fig. S6). While the trends observed were identical to previous investigations by Mössbauer spectroscopy [3], differences in ratios were evident. Such discrepancies may have reflected the limitations of fitting UV–Vis spectra, but also may have been influenced by the sample preparation for Mössbauer spectroscopy which relied on the quantification of complexes precipitated from solution. Equilibria existed [29] and precipitated compositions may not have accurately represented what was in solution. For comparison, plots of the absorption maximum for each cluster type are reported in Fig. S7.

We next attempted to apply spectral fitting to UV–Vis spectra acquired during cluster degradation. Here, the $[4Fe–4S]^{2+}$ cluster was coordinated to the peptide GCGGCGGGGC and incubated at different temperatures. This simple peptide contained the same spacing of cysteines as seen in the CX_2CX_4C motif of some types of radical SAM proteins, such as ThiC [30]. As this peptide only contained three cysteines, the peptide coordinated the iron-sulfur cluster less stably. Such experiments can be difficult to monitor since the degraded species can absorb strongly. In fact, spectral fitting of $[4Fe–4S]^{2+}$ GCGGCGGGGC after incubation at 70 °C was poor with a reference library consisting solely of $[1Fe–0S]^{2+}$, $[2Fe–2S]^{2+}$, and $[4Fe–4S]^{2+}$ clusters (Fig. 3A, Fig. S8). To improve fitting and to account for the released components of the degraded cluster, spectra of non-metallated peptide and of solutions under identical conditions in the presence of iron and hydrosulfide ions but in the absence of peptide were included in the reference library. Fits with the three peptidyl clusters in addition to the non-metallated peptide and the non-peptidyl iron sulfide gave a model spectrum that represented well the experimental spectrum (Fig. 3B, Fig. S9). If only individual absorption bands indicative of each cluster type were used to monitor the sample from 25 °C to 70 °C, the data would not be easily interpretable, since absorption increased for the bands indicative of $[1Fe–0S]^{2+}$, $[2Fe–2S]^{2+}$, and $[4Fe–4S]^{2+}$ clusters (Fig. 3C). Conversely, spectral fitting at each temperature with the full reference library were clear. The $[4Fe–4S]^{2+}$ cluster degraded into non-peptidyl iron sulfide complexes and not peptide bound iron-sulfur clusters of lower nuclearity at temperatures above 60 °C (Fig. 3D).

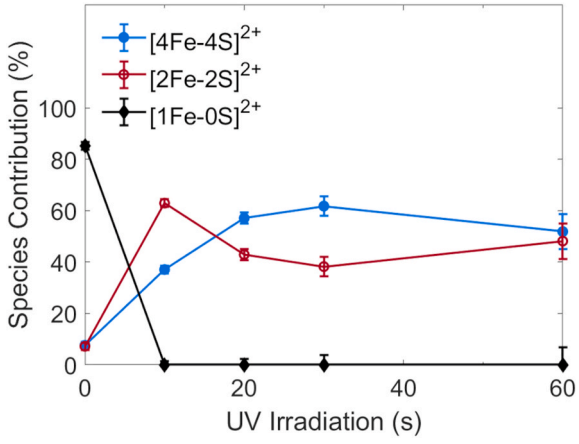

Fig. 2. Time-dependent changes of iron-sulfur glutathione. A solution of 40 mM glutathione, 0.4 mM $FeCl_3$, pH 8.7 was irradiated with UV light, and absorption spectra were collected and fit to a spectral library of $[1Fe–0S]^{2+}$, $[2Fe–2S]^{2+}$, and $[4Fe–4S]^{2+}$ peptides.

Finally, to demonstrate that the reference spectra were capable of accurately identifying the presence of $[2Fe–2S]^{2+}$ clusters, as such iron-sulfur clusters are rarer, we next tested glutathione under conditions known to give rise to $[2Fe–2S]^{2+}$ cluster [31]. The anaerobic addition of 0.19 mM Na_2S and 0.4 mM $FeCl_3$ to 40 mM glutathione showed the immediate assembly of $[2Fe–2S]^{2+}$ cluster (Fig. 4, Fig. S10). Monitoring the solution at single wavelengths failed to distinguish well between the $[2Fe–2S]^{2+}$ and $[4Fe–4S]^{2+}$ clusters (Fig. S11).

3.3. Limitations

Fit-FeS can only provide a semi-quantitative snapshot of reaction solutions. Mixtures of iron-sulfur clusters will always be difficult to parse, and other spectroscopic techniques are superior for the quantification and investigation of nuclear and electronic transitions. Further, the same type of iron-sulfur cluster ligated by different scaffolds will show small differences in their respective absorption spectra, which further complicates spectral decomposition. Conversely, iron-sulfur clusters typically show a band near 310–315 nm irrespective of the nuclearity of the cluster. Therefore, discrimination between the different types of cluster can often be improved by restricting the spectral window to regions above 320 nm. Finally, [4Fe–4S] clusters absorb strongly and thus are capable of masking the presence of other types of clusters. This latter complication can be somewhat mitigated by a correction factor that takes into account the extinction coefficients of the characteristic peak for each cluster type, as provided by the tool described herein.

Fit-FeS does require some amount of user intervention to guide the process. A limitation of Solver is that the algorithm seeks a local minimum rather than a global minimum when reducing errors. Therefore, it is possible for Solver to get stuck at minima that do not best reflect the composition present in solution. Such situations require the user to alter the starting cluster ratios, perhaps iteratively, until good fits are obtained. Lastly, users should be cognizant of which bands reflect iron-

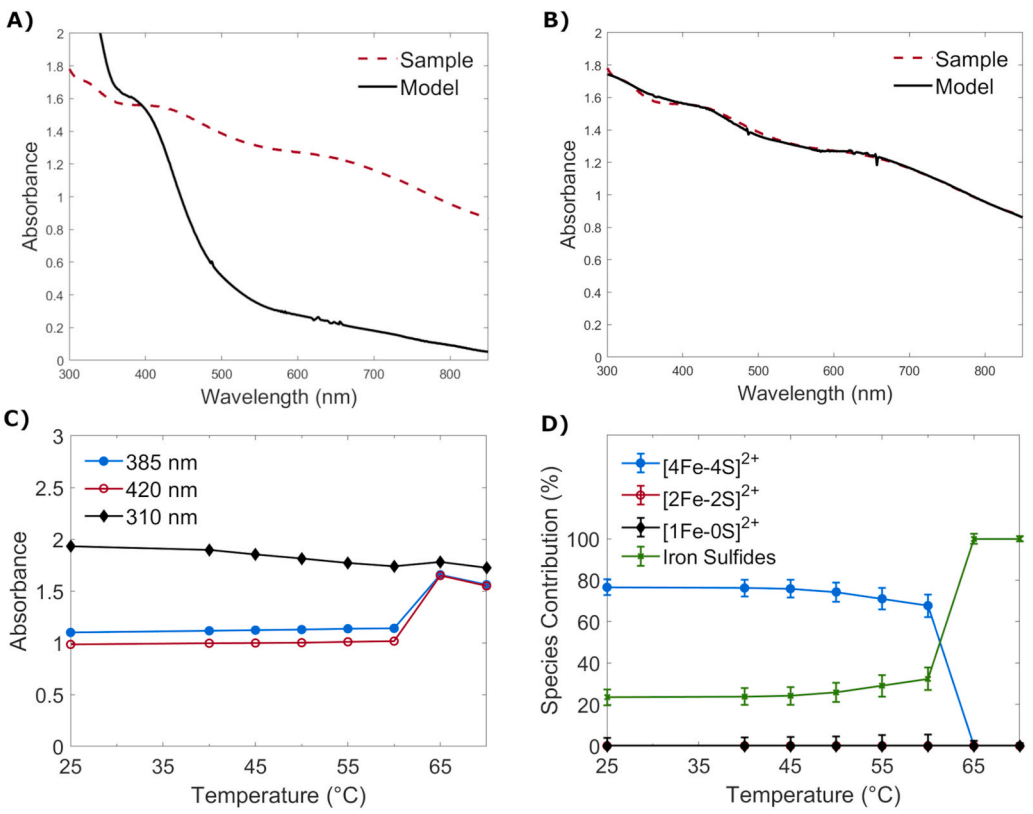

Fig. 3. Thermal stability of $[4Fe–4S]^{2+}$ GCGGCGGGGC. **A**) Spectral fitting of a sample incubated at 70 °C with a reference library consisting of $[4Fe–4S]^{2+}$, $[2Fe–2S]^{2+}$, and $[1Fe–0S]^{2+}$ clusters. **B**) Spectral fitting of a sample incubated at 70 °C with a reference library consisting of $[4Fe–4S]^{2+}$, $[2Fe–2S]^{2+}$, $[1Fe–0S]^{2+}$ clusters in addition to non-metallated peptide and non-peptidyl iron sulfide. Red (dashed line) spectra are experimentally collected, and black lines represent models generated by Fit-FeS. **C**) Temperature stability monitored at wavelengths diagnostic for each cluster type, including $[4Fe–4S]^{2+}$ (385 nm), $[2Fe–2S]^{2+}$ (420 nm), and $[1Fe–0S]^{2+}$ (310 nm) clusters. **D**) Species contribution obtained from Fit-FeS models. The conditions were 1.67 mM GCGGCGGGGC, 0.4 mM $FeCl_3$, and 0.8 mM Na_2S, 50 mM glycylglycine, pH 8.7. Samples were incubated at each temperature for 5 min prior to spectral acquisition. (For interpretation of the references to colour in this figure legend, the reader is referred to the Web version of this article.)

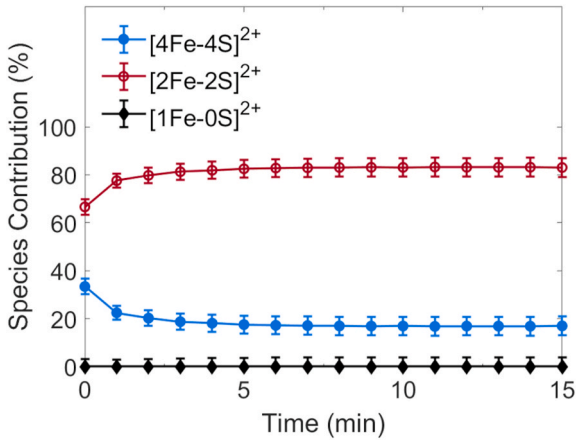

Fig. 4. The synthesis of $[2Fe–2S]^{2+}$ glutathione at pH 8.7. The final concentrations were 0.4 mM $Fe^{3+}_{(aq)}$, 0.19 mM HS^-, and 40 mM glutathione.

sulfur clusters and which are due to other species, such as protein bound organic chromophores, and adjust the spectral window accordingly. Despite these limitations, UV–vis spectroscopy has long been and will continue to be an important tool for the investigation of iron-sulfur clusters for the foreseeable future. We are hopeful that Fit-FeS will facilitate analyses of one of life's most ancient cofactors.

Declaration of competing interest

The authors declare no conflict of interests.

Acknowledgments

We thank D. Rossetto, L. Valer, Y. J. Hu, and F. Connolly for comments on the manuscript and for testing Fit-FeS.

Appendix A. Supplementary data

Supplementary data to this article can be found online at https://doi.org/10.1016/j.ab.2021.114269.

CRediT author statement

Isaiah O. Betinol: Conceptualization, Methodology, Software, Writing. **Serge Nader:** Conceptualization, Methodology, Software, Writing. **Sheref S. Mansy:** Conceptualization, Supervision, Funding acquisition, Writing.

Funding

We acknowledge the support of the Simons Foundation (290358FY19 and 651656) and the Natural Sciences and Engineering Research Council of Canada (NSERC) [RGPIN-2020-04375] to S.S.M.

References

[1] H. Beinert, Iron-sulfur proteins: ancient structures, still full of surprises, JBIC J. Biol. Inorg. Chem. 5 (1) (2000) 2–15, https://doi.org/10.1007/s007750050002.
[2] A. Galambas, J. Miller, M. Jones, E. McDaniel, M. Lukes, H. Watts, V. Copié, J. B. Broderick, R.K. Szilagyi, E.M. Shepard, Radical S-adenosylmethionine maquette chemistry: cx3Cx2C peptide coordinated redox active [4Fe–4S] clusters, JBIC J. Biol. Inorg. Chem. 24 (6) (2019) 793–807, https://doi.org/10.1007/s00775-019-01708-8.
[3] C. Bonfio, L. Valer, S. Scintilla, S. Shah, D.J. Evans, L. Jin, J.W. Szostak, D. D. Sasselov, J.D. Sutherland, S.S. Mansy, UV-Light-Driven prebiotic synthesis of iron–sulfur clusters, Nat. Chem. 9 (12) (2017) 1229–1234, https://doi.org/10.1038/nchem.2817.
[4] S.A. Sanden, R. Yi, M. Hara, S.E. McGlynn, Simultaneous synthesis of thioesters and iron–sulfur clusters in water: two universal components of energy metabolism, Chem. Commun. 56 (80) (2020) 11989–11992, https://doi.org/10.1039/D0CC04078A.

[5] R.H. Holm, W. Lo, Structural conversions of synthetic and protein-bound iron–sulfur clusters, Chem. Rev. 116 (22) (2016) 13685–13713, https://doi.org/10.1021/acs.chemrev.6b00276.
[6] SigmaPlot; Systat Software: San Jose, California.
[7] A|e - UV-Vis-IR Spectral Software 1.2; FluorTools, www.fluortools.com.
[8] MATLAB®; MathWorks Inc.: Natick, (Massachusetts, USA).
[9] R Core Team. R, A Language and Environment for Statistical Computing, R Foundation for Statistical Computing, Vienna, Austria, 2017.
[10] D. Fylstra, L. Lasdon, J. Watson, A. Waren, Design and use of the Microsoft Excel solver, Interfaces 28 (5) (1998) 29–55, https://doi.org/10.1287/inte.28.5.29.
[11] D.C. Harris, Nonlinear least-squares curve fitting with Microsoft Excel solver, J. Chem. Educ. 75 (1) (1998) 119, https://doi.org/10.1021/ed075p119.
[12] E.J. Billo, Excel for Chemists: A Comprehensive Guide, third ed., Wiley, Hoboken, N.J, 2011.
[13] R. de Levie, How to Use Excel® in Analytical Chemistry: and in General Scientific Data Analysis, Cambridge University Press, 2001.
[14] J.D.A. Parsons, High-throughput method for fitting dose–response curves using Microsoft Excel, Anal. Biochem. 360 (2) (2007) 309–311, https://doi.org/10.1016/j.ab.2006.09.033.
[15] G. Kemmer, S. Keller, Nonlinear least-squares data fitting in Excel spreadsheets, Nat. Protoc. 5 (2) (2010) 267–281, https://doi.org/10.1038/nprot.2009.182.
[16] A. Owczarek, M.A. Olszewska, Development and validation of UHPLC-PDA method for simultaneous determination of bioactive polyphenols of horse-chestnut bark using numerical optimization with MS Excel solver, J. Pharmaceut. Biomed. Anal. 190 (2020) 113544, https://doi.org/10.1016/j.jpba.2020.113544.
[17] S.E. Mulholland, B.R. Gibney, F. Rabanal, P.L. Dutton, Characterization of the fundamental protein ligand requirements of [4Fe-4S] $^{2+/+}$ clusters with sixteen amino acid maquettes, J. Am. Chem. Soc. 120 (40) (1998) 10296–10302, https://doi.org/10.1021/ja981279a.
[18] T. Chai, R.R. Draxler, Root mean square error (RMSE) or mean absolute error (MAE)? – arguments against avoiding RMSE in the literature, Geosci. Model Dev. (GMD) 7 (3) (2014) 1247–1250, https://doi.org/10.5194/gmd-7-1247-2014.
[19] M. Nakata, N. Ueyama, T. Terekawa, A. Nakamura, Oxidized rubredoxin models. II. Iron (III) complexes of Z-cys-pro-leu-cys-OMe and Z-cys-thr-val-cys-OMe, Bull. Chem. Soc. Jpn. 56 (1983) 3647–3651.
[20] N. Ueyama, S. Ueno, A. Nakamura, K. Wada, H. Matsubara, S.-I. Kumagai, S. Sakakibara, T. Tsukihara, A synthetic analogue for the active site of plant-type ferredoxin: two different coordination isomers by a four-cys-containing [20]-Peptide, Biopolymers 32 (11) (1992) 1535–1544, https://doi.org/10.1002/bip.360321111.
[21] M.L. Kennedy, B.R. Gibney, Proton coupling to [4Fe-4S] $^{2+/+}$ and [4Fe-4Se] $^{2+/+}$ oxidation and reduction in a designed protein, J. Am. Chem. Soc. 124 (24) (2002) 6826–6827, https://doi.org/10.1021/ja0171613.
[22] K.S. Hagen, A.D. Watson, R.H. Holm, Synthetic routes to iron sulfide (Fe2S2, Fe3S4, Fe4S4, and Fe6S9), clusters from the common precursor tetrakis (Ethanethiolate)Ferrate(2-) ion ([Fe(SC2H5)4]2-): structures and properties of [Fe3S4(SR)4]3- and bis(Ethanethiolate)Nonathioxohexaferrate(4-) ion ([Fe6S9 (SC2H5)2]4-), examples of the newest types of Fe-S-sr clusters, J. Am. Chem. Soc. 105 (12) (1983) 3905–3913, https://doi.org/10.1021/ja00350a028.
[23] D. Rickard, G.W. Luther, Chemistry of iron sulfides, Chem. Rev. 107 (2) (2007) 514–562, https://doi.org/10.1021/cr0503658.
[24] S.S. Leal, C.M. Gomes, Linear three-iron centres are unlikely cluster degradation intermediates during unfolding of iron-sulfur proteins, Biol. Chem. 386 (12) (2005), https://doi.org/10.1515/BC.2005.147.
[25] S.E. Mulholland, B.R. Gibney, F. Rabanal, P.L. Dutton, Determination of nonligand amino acids critical to [4Fe-4S] $^{2+/+}$ assembly in ferredoxin maquettes †, Biochemistry 38 (32) (1999) 10442–10448, https://doi.org/10.1021/bi9908742.
[26] P.V. Rao, R.H. Holm, Synthetic analogues of the active sites of Iron−Sulfur proteins, Chem. Rev. 104 (2004) 527–559.
[27] R. Hanscam, E.M. Shepard, J.B. Broderick, V. Copié, R.K. Szilagyi, Secondary structure analysis of peptides with relevance to iron–sulfur cluster nesting, J. Comput. Chem. 40 (2) (2019) 515–526, https://doi.org/10.1002/jcc.25741.
[28] A. Hoppe, M.-E. Pandelia, W. Gärtner, W. Lubitz, [Fe4S4]- and [Fe3S4]-cluster formation in synthetic peptides, Biochim. Biophys. Acta BBA - Bioenerg 1807 (11) (2011) 1414–1422, https://doi.org/10.1016/j.bbabio.2011.06.017.
[29] S. Scintilla, C. Bonfio, L. Belmonte, M. Forlin, D. Rossetto, J. Li, J.A. Cowan, A. Galliani, F. Arnesano, M. Assfalg, S.S. Mansy, Duplications of an iron–sulphur tripeptide leads to the formation of a protoferredoxin, Chem. Commun. 52 (92) (2016) 13456–13459, https://doi.org/10.1039/C6CC07912A.
[30] A. Chatterjee, Y. Li, Y. Zhang, T.L. Grove, M. Lee, C. Krebs, S.J. Booker, T.P. Begley, S.E. Ealick, Reconstitution of ThiC in thiamine pyrimidine biosynthesis expands the radical SAM superfamily, Nat. Chem. Biol. 4 (12) (2008) 758–765, https://doi.org/10.1038/nchembio.121.
[31] W. Qi, J. Li, C.Y. Chain, G.A. Pasquevich, A.F. Pasquevich, J.A. Cowan, Glutathione complexed Fe–S centers, J. Am. Chem. Soc. 134 (26) (2012) 10745–10748, https://doi.org/10.1021/ja302186j.